High precision fiber-optic gyro with extended dynamic range

Yu.N. Korkishko[1,2] , V.A.Fedorov[1,2], V.E.Prilutskiy[1,2], V.G.Ponomarev[1] , I.V.Morev[1], D.V.Obuhovich[1,2], S.M.Kostritskii[1,2] , I.V.Fedorov[1], A.I.Zuev[1,2], V.K.Varnakov[1,2]
[1] Optolink RPC LLC,
Moscow, Russia
opto@optolink.ru
[2] Fiber Optical Solution,
Riga, Latvia
korkishko@fiberopticalsolution.lv

***Abstract*— At present time fiber-optic gyroscopes (FOGs) with closed-loop feedback scheme of operation are becoming widely used in inertial navigation systems. One of the main restrictions on FOG usage in the applications of inertial navigation is the limited range of measured angular rate (dynamic range). In this paper we present the results of the new high-precision FOG SRS-1001 development and test results. SRS-1001 FOG, which is the modification of serial SRS-1000 FOG, allows to overcome the observed restrictions and shows the extended dynamic range of 1000 °/s, compared with the dynamic range of 90 °/s for the standard SRS-1000. Furthermore, SRS-1001 has the potential of further dynamic range increase up to 2000 °/s with the retention of high scale factor stability in overall measurement range.**

Keywords*— *fiber-optic gyroscope, dynamic range

I. INTRODUCTION

At present time fiber-optic gyroscopes (FOGs) with closed-loop feedback scheme of operation are becoming widely used in inertial navigation complexes [1-2]. In FOGs with closed-loop scheme the feedback mechanism keeps the zero signal level by compensating the Sagnac phase shift with additional phase counter-shift. The value of the phase counter-shift allows one to obtain information about the angular rate of the device rotation. One of the serious restrictions on FOG applications in inertial navigation comes from their restricted angular rate measurement range. For serially produced precision FOG SRS-1000, precision class 0.005°/h, with fiber coil length and diameter 1000 m and 140 mm, respectively, the angular rate measurement range (dynamic range) comprises 90 °/s. The rotation rate sign keeping range for the same device is 180 °/s. For various applications that need both the precision and the correct measurement of high rotation rates up to 300 °/s and even more, the need for SRS-1000 dynamic range extension is evident.

In this paper we present the results for new FOG SRS-1001, designed on the basis of serial SRS-1000, in which the described restrictions are overcome.

II. FIBER-OPTIC GYROSCOPES

All FOGs produced by Optolink RPC and "Fiber Optical Solution" (FOS) are made in co-called minimum configuration with digital signal processing (DSP) [3-11]. Minimum configuration ensures the reciprocity of optical paths for two beams counter-propagating in a fiber loop.

Structural scheme of single-axis FOGs with DSP is represented in Figure 1. FOGs consist of one light source with central wavelength 1550 nm, one photodetectors, one fiber splitter (1:1) to divide the light wave into two parts, one ring interferometer to sense angular rate, and signal processing circuits [3-11]. Ring interferometer consists of a multifunction integrated optic chip (MIOC) and polarization maintaining (PM) fiber coil with the length of 1000 meters (for SRS-1000), also produced by Optolink. The MIOC is a three-port integrated optical chip fabricated at lithium niobate wafer which executes three functions [3]. DSP generates voltage for "sawtooth" light modulation in order to compensate Sagnac phase shift and to make fixed phase shift $\pi/2$ between counter-propagating waves using additional modulation. As a result, each channel is operating in closed-loop regime [4-11].

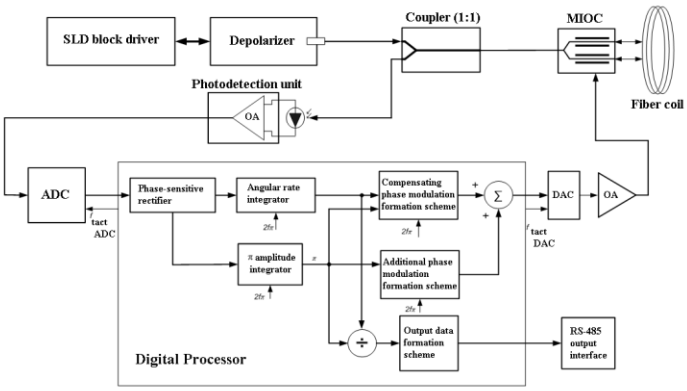

Fig. 1. FOG SRS-1000 structural scheme

where SLD – light source, superluminescent light emitting diode; MIOC – multifunctional integrated optic chip; OA – operational amplifier, ADC – analog-to-digital converter, DAC – digital-to-analog converter, RS-485 – serial interface.

SRS-1001 utilizes the scheme that includes closed-loop feedback scheme for rotation rate measurement. The output rotation rate is proportion to the incline angle of applied compensating phase modulation, the amplitude of which is kept at 2π rad value.

It is widely known that the dependence of the light intensity at the photodiode on the rotation rate of the fiber coil shows cosine nature, however, the number of periods could be exceedingly large. Standing at the point, corresponding to the Sagnac phase shift of 2π rad (as in the case of FOG switch on in conditions of rotation with the rate, making the compensation phase shift around 2π rad), FOG will measure the value $\Omega_{\Delta\varphi}$ rad, but not the correct rotation rate value $\Omega_{2\pi}$ + $\Omega_{\Delta\varphi}$ rad (Figure 2).

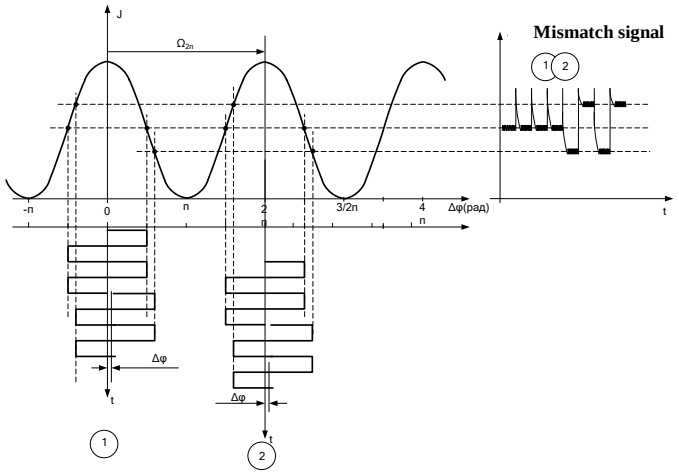

Fig. 2. Scheme of FOG output signal formation

The value of rotation rate $\Omega_{2\pi}$ is calculated using the compensating modulation phase amplitude. Thus, in order to measure the true rotation rate, one needs to identify the half-period number in which the Sagnac phase shift is located.

At the first stage, we developed the processing scheme that allows to measure angular rate more than 1000°/s on condition that FOG is switched on at rates lower than 90°/s. It works the following way: the scheme automatically resets the integrator, changes the sign on the input of the integrator, and adds on the output the value of angular rate Ωπ in the case of reaching the angular rate corresponding to phase shift multiple to π rad. The scheme of the device corresponding to this version is displayed in Figure 3.

The description for the operation of dynamic range extension scheme is provided below:

Code, proportional to the angular rate of device rotation, comes from angular rate integrator (3) and proceeds to the scheme of dynamic range extension into comparators (9), (10) and adder (14). Trigger thresholds for comparators (9), (10) are formed using the code obtained from the compensating phase modulation amplitude integrator(2). The code corresponds to the value of angular rate that produces the Sagnac phase shift in the interferometer equal to π rad.

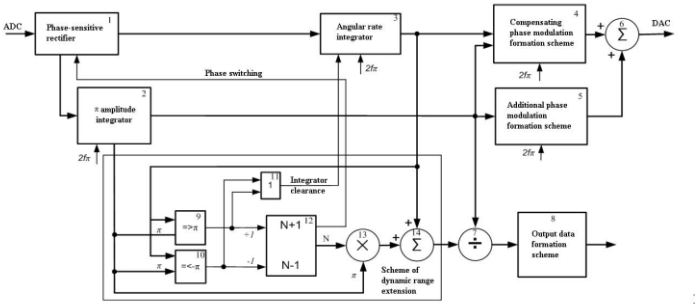

Fig. 3. FOG digital processing scheme with extended dynamic range where 6 – summator for phase modulation code formation, 7 – divisor of angular rate on compensating phase modulation code, 9, 10 – comparator, 11 - scheme «OR», 12 – half-period counter, 13 - multiplier, 14 – adder.

Comparator (9) is only for the positive values of angular rate integrator output signal (3); comparator (10) – only for negative values. In case of reaching the angular rate that corresponds to the phase shift equal to π rad (π-phase-shift angular rate) or more, comparator (9) sends the signal of increasing by 1 the counter of π-rad-transitions number (half-period counter) (12) value . In case of reaching the angular rate that corresponds to the phase shift equal to -π rad or less, comparator (10) sends the signal of decreasing by 1 the value of half-period counter (12).

Signals from comparators (9), (10) are also sent to scheme «OR» (11), in which the angular rate integrator clearance signal (3) is formed. Half-period counter (12) forms the signed value N that corresponds to the sum of comparators (9) and (10) signals. In case of an odd value of half-period counter (12) the phase switch signal is produced in phase-sensitive rectifier (1).

Half-period counter value is sent to multiplier (13), in which it is multiplied by the value of π-phase-shift angular rate. Multiplication result is send into the adder (14), where it is added to the angular rate value from angular rate integrator (3). The resulting value from the adder goes to the divisor (7) for correction on amplitude π.

FOG SRS-1000 tests with such processing scheme showed the scale factor linearity retention up to angular rates ±1000°/s with reliable measurement range switching. The results for the developed FOG SRS-1001 with extended dynamic range are presented in Figures 4-6. SRS-1001 output signal during the stepwise angular rate change in range 10-540 °/s (in single launch) is shown in Figure 4. Calculated results of two produced and tested SRS-1001 devices in similar launches are shown in Figure 5. These results confirm high scale factor stability (less than 50 ppm) in overall extended angular rate measurement range (up to 550 °/s).

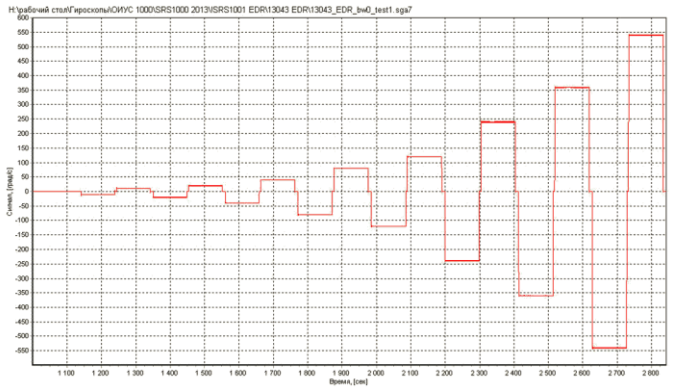

Fig. 4. SRS-1001 output signal during the stepwise angular rate change in range 10-540 °/s in single launch

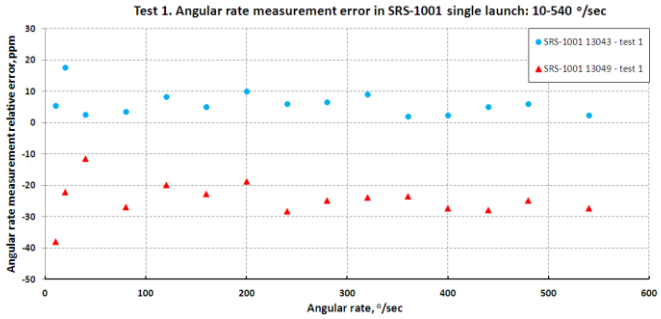

Fig. 5. Angular rate measurement relative error of two SRS-1001 devices during the stepwise angular rate change in range 10-540 °/s in single launch

Fig. 6 shows the results of testing SRS-1001 units in single launch on the border of two octaves (angular rate value ~90 °/s, corresponding to the phase shift multiple to π rad.) – results confirm that the measurement on the border of two octaves does not affect SRS-1001 parameters, no difference in characteristics is observed.

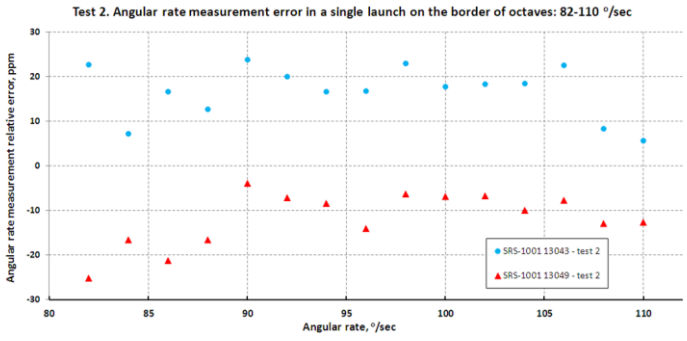

Fig. 6. Angular rate measurement relative error in a single launch on the border of two octaves

Nevertheless, there remained a problem with angular rates correct measurement in conditions of the FOG switch on at rates higher than 90°/s.

In order to solve this problem, we developed fiber-optic gyroscope SRS-1001, created on the basis of FOG SRS-1000 optical scheme. For the identification of the half-period number in which Sagnac phase shift is located, SRS-1001 utilizes micromechanical (MEMS) gyro with angular rate measurement range more than 1000°/s. FOG digital processing scheme with MEMS gyroscope correction is shown in Figure 7.

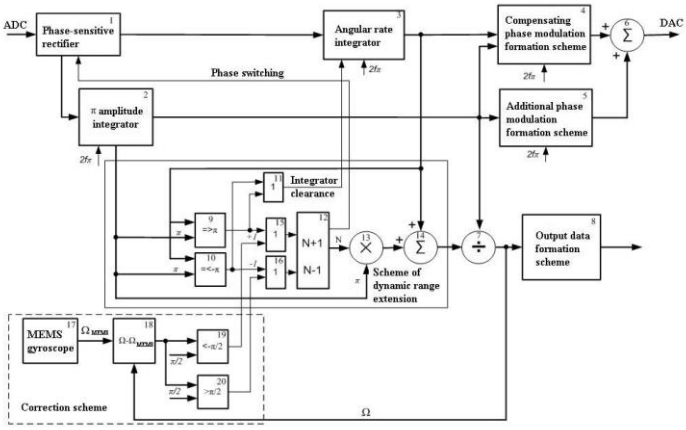

Fig. 7. FOG digital processing scheme with MEMS gyroscope correction and extended dynamic range

The description for the operation of dynamic range extension scheme with MEMS correction is provided below:

Angular rate value, measured with MEMS gyroscope (17), is subtracted in the scheme of subtraction (18) from the angular rate value measured by FOG. The obtained value of difference is compared in comparators (19), (20) with the angular rate value that corresponds to π phase shift. If the difference is less than -π rad, the signal is sent to increase by 1 the value of half-period counter (12), which passes through scheme «OR» (15). If the difference is greater than π rad, the signal is sent to decrease by 1 the value of half-period counter (12), which passes through scheme «OR» (16).

The results of SRS-1001 angular rate measurement error calculation for the tests with SRS-1001 switching on in rotation, presented in Figure 8, show the correctness of the developed scheme that utilizes MEMS gyroscope for counting the amount of output signal half-periods. In addition, the results show that the accuracy (scale factor stability) does not depend on switch-on conditions (with or without FOG rotation at the moment of switching).

Figure 9 shows the results of SRS-1001 angular rate measurement error calculation in run-to-run stability tests at rotation rate 100 °/s; devices were switched on in rotation. These results show that the scale factor stability values are almost equal for the cases of single launch tests and run-to-run tests.

The results of FOG SRS-1001 bias and temperature drift stability tests at stable temperatures +20°C, -30°C and +60°C, and also in conditions of gradual temperature change in range -30°C - +60°C have shown that SRS-1001 devices with extended dynamic range up to 550°/s retain all accuracy parameters of FOG SRS-1000.

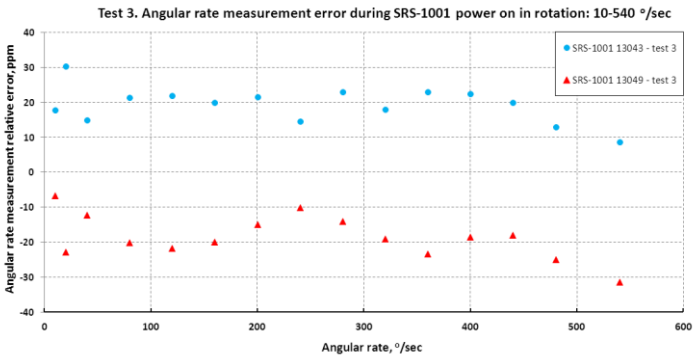

Fig. 8. SRS-1001 angular rate measurement error in tests with switching on in rotation

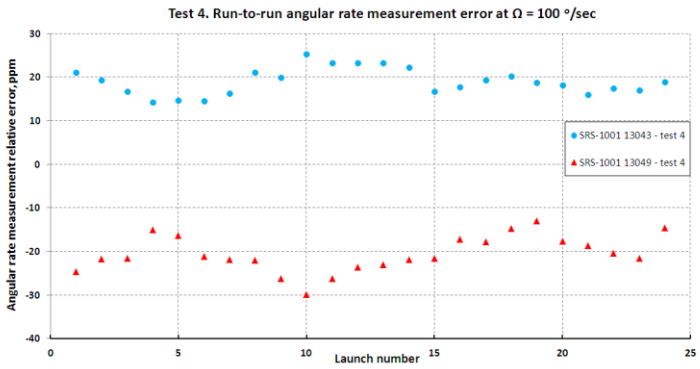

Fig. 9. SRS-1001 run-to-run angular rate measurement error at rotation rate 100°/s

Figure 10 presents SRS-1001 angular rate measurement error in range up to 600°/s at temperatures -30°C, +20°C and +60°C. These results confirm high scale factor stability (less than 50 ppm) in overall extended angular rate measurement range and overall temperature range.

Figure 11 presents Allan variance plots for FOG SRS-1001 devices, previously measured for compliance with specified scale factor stability parameters. Comparison of FOGs parameters - Bias Instability (Drift) and Angle Random Walk, calculated according to international (Allan variance method) and russian domestic standards, see in [12]. From the plots we can see that the devices also fully meet the specifications for Bias Drift and ARW accuracy parameters.

Final accuracy and operational characteristics (specification) of developed high-precision fiber-optic gyroscope SRS-1001 with extended dynamic range are summarized in Table 1.

Figure 12 presents the image of produced and tested for accuracy parameters FOG SRS-1001 with extended dynamic range.

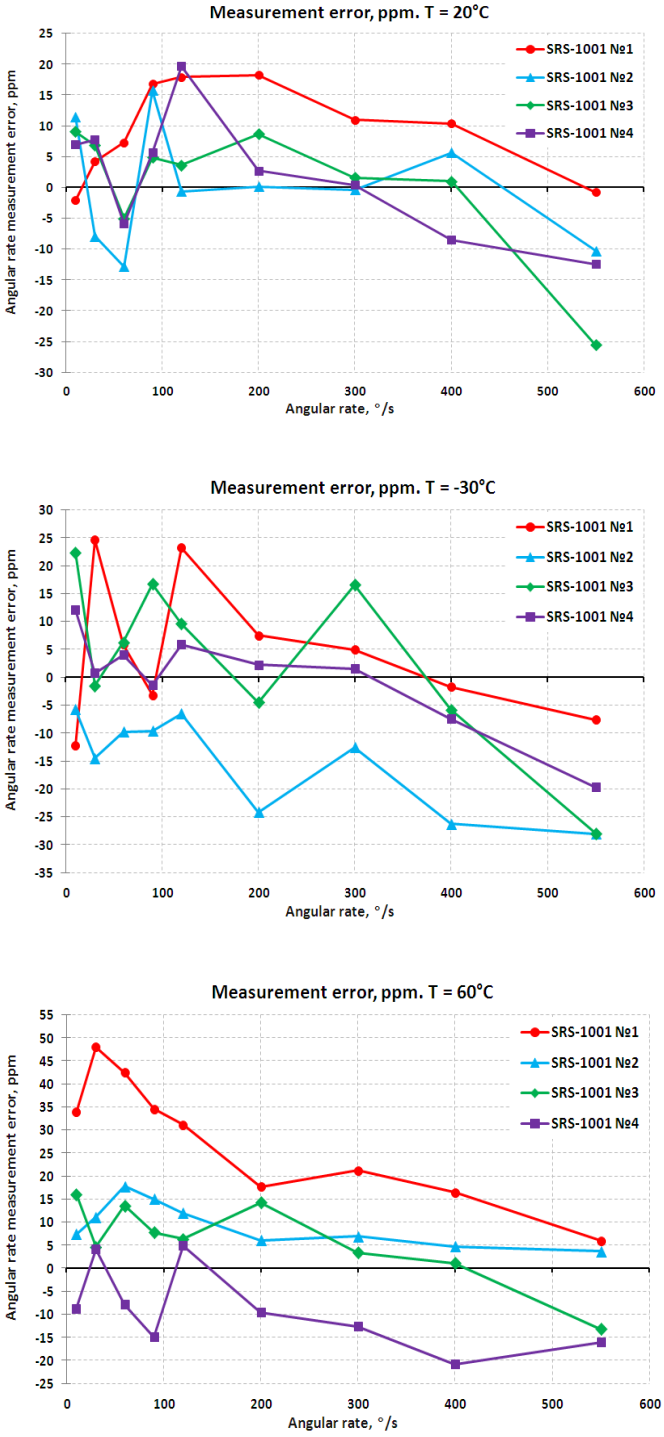

Fig. 10. SRS-1001 angular rate measurement error in range up to 600°/s at temperatures -30°C, +20°C and +60°C

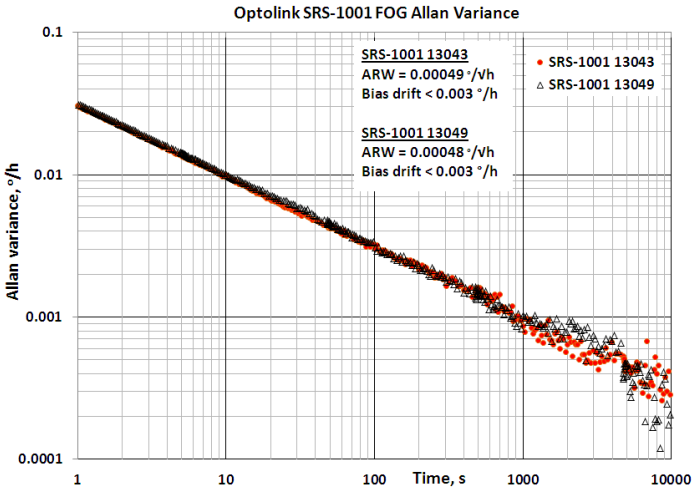

Fig. 11. Allan variance plots for FOG SRS-1001 devices

TABLE I. ACCURACY AND OPERATIONAL CHARACTERISTICS OF HIGH-PRECISION FIBER-OPTIC GYROSCOPE SRS-1001 WITH EXTENDED DYNAMIC RANGE

Parameter	Single axis FOG SRS-1001
Range of measured angular rate, °/s	±1000
Bias Drift at fixed temperature, °/h	≤0.005
Scale factor repeatability, ppm	≤200
Bandwidth, Hz:	100
Angle Random walk (ARW), °/√h	≤0.0005
Weight, kg	0.8
Dimensions, mm	Ø150×80
Output signal	RS-485

Fig. 12. Image of FOG SRS-1001 with extended dynamic range

Hence, companies Optolink RPC LLC and SIA "Fiber Optical Solution" have developed and manufactured the new high-precision fiber-optic gyro with extended range of measured angular rates, which have passed all preproduction tests. These gyros display high stability of scale factor in overall measurement range.

REFERENCES

[1] Lefevre H., The Fiber-Optic Gyroscope, Artech House, 1993.

[2] Optical fiber rotation sensing, edited by W.K.Burns, Academic press, 1994.

[3] Yu.N.Korkishko, V.A.Fedorov, S.M.Kostritskii, A.N.Alkaev, E.M. Paderin, E.I.Maslennikov, D.V.Apraksin. Multifunctional integrated optical chip for fiber optical gyroscope fabricated by high temperature proton exchange // in Proceedings of SPIE, Vol.4944, Integrated Optical Devices: Fabrication and Testing, edited by Giancarlo C. Righini, (SPIE, Bellingham, WA, 2003), pp. 262-267.

[4] Korkishko, Yu.N., Fedorov, V.A., Prilutskii, V.E., Ponomarev, V.G., Fenyuk, M.A., Marchuk, V.G., Kostritskii, S.M., and Paderin, E.M., High-precision fiber-optic gyroscope with a linear digital output, Giroskopiya i Navigatsiya, 2004, no. 1, pp. 69–82.

[5] Prilutskii, V.E., Ponomarev, V.G., Marchuk, V.G, Fenyuk, M.A., Korkishko, Yu.N., Fedorov, V.A., Kostritskii, S.M., Kostritskii, S.M., Paderin, E.M., and Zuev A.I., Interferometric fiber-optic gyroscopes witha linear digital output, Giroskopiya i Navigatsiya, 2004, no. 3 , pp. 62–72.

[6] Yu.N. Korkishko, V.A. Fedorov, V.E. Prilutskii, V.G. Ponomarev, V.G.Marchuk, I.V.Morev, E.M. Paderin, S.M.Kostritskii, V.N.Branets, V.S.Ryzhkov. Space grade three-axis fiber optical gyroscope // in Proc. EOS Topical Meeting on Photonic Devices in Space, October 18-19, 2006, Paris, France. Vol.5, pp.32-35.

[7] Korkishko, Yu.N., Fedorov, V.A., Prilutskii, V.E., Ponomarev, V.G., Marchuk, V.G., Morev, I.V., Paderin, E.M., Kostritskii, S.M., Paderin, Nesenyuk, L.P., Buravlev, A.S., and Lisin, L.G., Navigation grade fiber optical gyroscope, Giroskopiya i Navigatsiya, 2008, no. 1, pp.71-81.

[8] Yu.N. Korkishko, V.A.Fedorov, V.E.Prilutskii, V.G.Ponomarev, I.V.Morev, S.M.Kostritskii. Interferometric closed-loop fiber-optic gyroscopes // in Proceedings of SPIE, Vol.8351, Third Asia Pacific Optical Sensors Conference, edited by John Canning, Gangding Peng, (SPIE, Bellingham, WA, 2012), 83513L, pp. 83513L-1–83513L-8 (2012).

[9] Yu.Korkishko, V.Fedorov, V.Prilutskii, V.Ponomarev, I.Morev, S. Kostritskii, A.Zuev, V.Varnakov. Closed loop fiber optical gyroscopes for commercial and space applications // in Proc. Inertial Sensors and Systems - Symposium Gyro Technology 2012, Karlsruhe, Germany, 18-19 September 2012, p.14.1-14.15.

[10] Yu.N.Korkishko, V.A.Fedorov, V.E.Prilutskii, V.G.Ponomarev, I.V.Morev, S.M.Kostritskii, A.I.Zuev, V.K.Varnakov. Interferometric closed loop fiber optical gyroscopes for commercial and space applications // in Proceedings of SPIE, Vol.8421, OFS2012 22nd International Conference on Optical Fiber Sensors, edited by Yanbiao Liao, Wei Jin, David D. Sampson, Ryozo Yamauchi, Youngjoo Chung, Kentaro Nakamura, Yunjiang Rao, (SPIE, Bellingham, WA, 2012), 842107, pp. 842107-1–842107-8 (2012).

[11] Yu.N.Korkishko, V.A.Fedorov, V.E.Prilutskiy, V.G.Ponomarev, I.V.Morev, D.V.Obuhovich, I.V.Fedorov, N.I.Krobka. Investigation and Identification of Noise Sources of High Precision Fiber Optic Gyroscopes// in Proc. 20th Saint Petersburg International Conference on Integrated Navigation Systems, Saint Petersburg, May 27-29, 2013, pp.59-62.

[12] Yu.N.Korkishko, V.A.Fedorov, V.E.Prilutskii, V.G.Ponomarev, I.V.Morev, S.F.Skripnikov, M.I.Khmelevskaya, A.S.Buravlev, S.M.Kostritskii, I.V.Fedorov, A.I.Zuev, V.K.Varnakov. Strapdown Inertial Navigation Systems Based on Fiber Optic Gyroscopes // Gyroscopy and Navigation, 2014, Vol. 4, No. 4, pp. 195–204.